

## Simulation of the decomposition of di-cumyl peroxide in an ARSST unit

E. Marco, S. Cuartielles, J.A. Peña, J. Santamaria\*

*Department of Chemical and Environmental Engineering, Faculty of Science,  
University of Zaragoza, 50009 Zaragoza, Spain*

Received 28 February 2000; accepted 20 June 2000

### Abstract

The decomposition of di-cumyl peroxide (DCP) has been carried out in a commercial reaction calorimeter (ARSST<sup>TM</sup>), under near-adiabatic reaction conditions. The decomposition was then simulated by means of a simple model which used kinetics derived from concentration–time data obtained in isothermal experiments. This method allowed a more precise determination of the activation energy and pre-exponential factor for DCP decomposition. The model developed was able to predict with good accuracy the main characteristics of the decomposition process, and was also used to investigate the sensitivity of the runaway with respect to the parameters values used in the simulation. © 2000 Elsevier Science B.V. All rights reserved.

*Keywords:* Runaway; Thermal explosion; Decomposition kinetics; Reactor safety

### 1. Introduction

Runaway reactions are among the most serious safety concerns in the chemical industry. This is due to their relative frequency and also to the severe consequences that may follow if a runaway accident leads to the rupture of the process vessel. In any reactor, where exothermic processes are taking place, maintaining a constant temperature requires a balance between the heat generation rate and the cooling capacity of the system. The imbalance between heat generation and heat removal may arise as a result of a number of incidents [1], such as the sudden (e.g. loss of cooling fluid due to a valve blockage) or gradual

(e.g. fouling of heat transfer surfaces) loss of cooling capacity, perturbations in the feed temperature and concentration of reactants, presence of impurities in the reactor feed, variations in the degree of mixing, accumulation of reactants or products, external events (e.g. external fire), development of hot spots in the reactor, etc. The higher temperature accelerates the chemical reaction, and therefore, the rate of heat generation which further increases the temperature, giving rise to the runaway phenomenon. One promising approach to solve this problem is the development of micro-reactors (see, e.g. Ref. [2]) where the ratio of surface area to reactor volume is several orders of magnitude higher than that of industrial reactors. Scale-up in this case consists in stacking a sufficiently large number of micro-units in parallel, which obviously carries a significant economic penalty. This probably restricts the micro-reactor approach

\* Corresponding author. Fax: +34-76-762142.  
E-mail address: iqcatal@posta.unizar.es (J. Santamaria).

to the small-scale production of highly hazardous chemicals.

It must be noticed that exothermic reactions are not exclusively limited to reactors. Undesired exothermic reactions (e.g. oxidation, reaction with water, decomposition of unstable substances) may take place in storage tanks or in process vessels other than reactors. In this case, very severe consequences are likely, since unwanted reactions are often not taken into account in the design of these vessels. Therefore, the temperature of the system must be kept below the maximum operating temperature, defined as the temperature at which the rate of exothermic reactions is still sufficiently low.

On an *a priori* basis, a clear divide between safe and unsafe operating temperatures does not exist, since the possibility of maintaining a constant temperature depends not only on the specific characteristics of the exothermic process (such as the reaction rate and heat of reaction), but also on the heat-transfer characteristics of the vessel. Thus, any temperature could in principle be used, provided that the heat transfer capability is sufficiently high. In general, however, this is not the case for industrial-size reactors, where the large volumes involved would require vast areas to confront the cooling requirements typical of a runaway process.

The current practice in processes where a runaway risk exists requires the determination of the boundaries for safe operation. An operating window can then be defined and implemented by means of adequate controls. Because the limits for safe operation are system-specific, their determination would ideally be carried out by simulating the dynamic behaviour of the reactor (or the process vessel) under study. However, this is seldom done, due to insufficient basic knowledge of the system (kinetics of the main reaction, thermodynamics, heat-transfer coefficients, secondary reactions, etc.). As a consequence, an experimental approach is favoured, in which the exothermic reaction is reproduced in the laboratory with the aim of determining the region of operability. As noted above, heat transfer is poor in large vessels, and this feature is approximated by carrying out the reaction under near-adiabatic conditions in special reactors designed to detect small temperature increments. This has given rise to the development of a new generation of commercial calorimeters (e.g. ARC<sup>TM</sup>,

RSST<sup>TM</sup>, ARSST<sup>TM</sup>, VSP<sup>TM</sup>, PhiTec<sup>TM</sup>, etc.) to determine the minimum operating temperature at which significant exothermic activity exists ( $T_{\text{onset}}$ ). The onset of exothermic activity is usually determined in screening experiments with these instruments as the moment when the measured temperature deviates from the temperature baseline. The sensitivity of this measurement depends not only on the design of the instrument, but also on the experimental conditions (sample size, baseline curvature) [3] and operating method (temperature ramp vs. heat–wait–search) used [4]. The data gathered enable the calculation of the parameters used to characterize runaway reactions: the onset temperature  $T_{\text{onset}}$ , the time to maximum rate (TMR), the maximum temperature  $T_{\text{max}}$  and the maximum rate of temperature increase  $(dT/dt)_{\text{max}}$  [5]. In a previous work [6], it was shown that  $T_{\text{onset}}$  can be determined with greater sensitivity by following the evolution of the gas-phase composition in systems where the runaway process gives rise to non-condensable gases.

It must be noticed that the above reaction calorimeters in fact measure temperature and then derive the heat generation rate from temperature–time data. In systems where only one reaction takes place the rate of heat generation is proportional to the rate of that particular reaction, and therefore temperature–time data have often been employed to calculate the kinetic parameters (apparent activation energy, pre-exponential factor, reaction order) of decompositions and other runaway reactions. These kinetics could then be used to predict the behaviour of the same reacting system in a different reactor or under a different set of conditions. Kossoy and Koludárova [7] pointed out the limitations of such temperature-based methods, which often lead to significant errors in the calculation of temperature evolution for larger scale systems.

This paper presents a simulation of the decomposition of di-cumyl peroxide (DCP) in a commercial calorimeter (ARSST<sup>TM</sup>). The kinetic parameters of the decomposition reaction were gathered from concentration–time data in isothermal experiments. These parameters are compared to those obtained from the fitting of the temperature–time data obtained in the ARSST<sup>TM</sup> during DCP decomposition and also to literature data. Finally, the influence of the kinetic parameters on  $T_{\text{onset}}$ ,  $T_{\text{max}}$ , TMR and  $(dT/dt)_{\text{max}}$  is discussed.

## 2. Experimental system and simulation model used

### 2.1. Experimental

The decomposition of DCP was investigated in isothermal experiments between 383 and 403 K. To this end, 16 glass ampoules were loaded with a small amount of a solution containing 40% DCP in ethylbenzene (EB). The ampoules were immersed vertically in a vigorously stirred bath of silicone oil at the desired temperature. About 40% of the volume of the 0.30-m long ampoules was out of the bath, acting as a condenser for DCP and EB vapours. Three glass ampoules were loaded with EB only and a thermocouple was inserted in order to monitor the temperature evolution. A fourth thermocouple was directly immersed in the silicone oil bath. The maximum temperature difference observed between the measuring points was 2 K. The glass ampoules were extracted at regular intervals, quenched in an ice bath and analyzed for peroxide concentration following the method of Zawadiak et al. [8].

In addition to the kinetic experiments, DCP decomposition experiments were carried out in an ARSST<sup>TM</sup> unit. In this case, 9 g of a solution of 40% DCP in EB were loaded in the ARSST<sup>TM</sup> glass test cell (typically  $\phi=1.04$ ). The unit was sealed and pressurized at room temperature with 2070 kPa-g of nitrogen. The sample was then heated at a rate of 1 K/min from room temperature to 358 K, then at 0.25 K/min from 358 to 573 K while following the evolution of the temperature inside the sample cell and the pressure above it. Unlike previous RSST<sup>TM</sup> models the ARSST<sup>TM</sup> has heat–wait–search capabilities, and is able to follow a prefixed temperature ramp under near-adiabatic conditions with great accuracy.

### 2.2. Model development

A simplified model was used to characterize the decomposition of DCP in the ARSST<sup>TM</sup> unit. The following assumptions were made:

Heat losses are negligible. All the energy input from the heating system is employed to heat the sample at a given heating rate.

The mass and volume of the liquid phase remain constant (i.e. evaporation losses can be neglected). The specific heat of the liquid can be considered as constant during the course of reaction.

A uniform temperature exists within the liquid phase.

The decomposition kinetics follow the expression given below (Eq. (3)), obtained from concentration–time data.

With these assumptions, the following heat balance can be written (a mass balance is not necessary, given the assumed stability of the liquid mass) as:

$$(-\Delta H_r)(-r_A)V + \phi m_l h_{sl} \left. \frac{dT}{dt} \right|_{set} = \phi m_l h_{sl} \frac{dT}{dt} \quad (1)$$

where  $-\Delta H_r$  is the heat of reaction (J/mol) obtained from the literature [10],  $-r_A$  the reaction rate (mol/m<sup>3</sup>s),  $V$  the liquid phase volume (m<sup>3</sup>),  $m_l$  and  $h_{sl}$  the mass (kg) and specific heat (in J/kg K, calculated using ASPEN Plus<sup>TM</sup> release 9.3 from Aspentech Inc.) of the liquid, respectively,  $dT/dt|_{set}$  the temperature ramp selected and  $\phi$  the thermal inertia coefficient, defined as

$$\phi = \frac{m_l h_{sl} + m_c h_{sc}}{m_l h_{sl}} \quad (2)$$

where  $m_c$  and  $h_{sc}$  correspond to the mass and specific heat of the glass sample cell used. After introducing the kinetics determined in concentration–time experiments, Eq. (1) was integrated using a 4th order Runge–Kutta–Gill routine to yield the variation of temperature with time. The reference values used in the simulation are given in Table 1.

## 3. Results and discussion

### 3.1. Kinetic experiments

Fig. 1 shows the DCP concentration–time curves obtained in the kinetic experiments at different tem-

Table 1  
Reference values used in the simulation of DCP decomposition

$E_a$ (J/mol)	$A_0$ (s <sup>-1</sup> )	$-\Delta H_r$ (J/mol)	$h_{sl}$ (J/g K)	$\phi$	$V$ (l)
147429	$2.08 \times 10^{15}$	290785	2.09	1.04	0.01

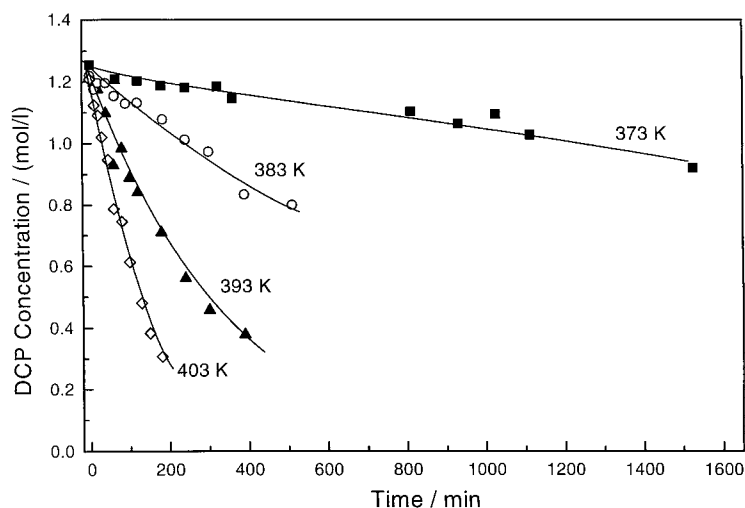


Fig. 1. DCP concentration vs. time in isothermal experiments.

peratures. The concentration–time data were fit to the equations given in Table 2 ( $C_A$  represents the peroxide concentration) using a commercial statistical package (Scientist<sup>TM</sup> 2.01 from Micromath). The first three equations in Table 2 are Arrhenius-type expressions with zero-, first- and second-order kinetics. The last two correspond to non-Arrhenius (auto-catalytic) equations; in these equations,  $x$  represents DCP conversion, and  $z$  can take values between 0.01 and 0.001 [9]. The first-order expression, gave the best fit ( $r=0.9985$ , Model Selection Criterion=3.2589, compared to 0.9973 and 2.6738, respectively, obtained with the second-order expression, which gave the second-best fit. This is in agreement with literature data [11] where a first-order reaction for the decomposition of DCP in benzene is reported. The apparent activation energy was  $35.3 \pm 0.7$  kcal/mol (147429 J/mol) and the pre-exponential factor  $2.08E+15 \pm 5.48E+13$  s<sup>-1</sup>. The kinetic equation describing

the decomposition of DCP in EB, obtained from concentration–time data is, therefore:

$$-r_A \equiv -\frac{dC_A}{dt} = 2.08 \times 10^{15} e^{-35300/RT} C_A \quad (3)$$

### 3.2. ARSST experiments: experimental results and simulation

The evolution of temperature for two ARSST<sup>TM</sup> experiments carried out under the same experimental conditions is presented in Fig. 2, together with the simulation results. It can be seen that the model predictions fall between both sets of experimental results, indicating that the model can predict  $T-t$  data with an accuracy comparable to the reproducibility of the ARSST<sup>TM</sup> experiments. The maximum temperature predicted is 16 K higher than that obtained experimentally, which was expected since the model does not take into account the small external heat losses that take place in the system or the heat consumption due to evaporation inside the ARSST<sup>TM</sup> chamber.

The slope of the Arrhenius plots in Fig. 3 is slightly higher for the experimental curves, indicating a higher activation energy. In fact, the activation energy calculated from the experimental data of Fig. 3 is 38.3 kcal/mol (vs. 35.3 kcal/mol obtained from the concentration–time experiments). Although the difference is small (ca. 10%), the fact that a higher

Table 2

Equations used to fit concentration–time data during DCP decomposition

Eq. No.	Equation
(1)	$-r_A \equiv -dC_A/dt = k$
(2)	$-r_A \equiv -dC_A/dt = kC_A$
(3)	$-r_A \equiv -dC_A/dt = kC_A^2$
(4)	$-r_A \equiv -dC_A/dt = -C_{A_0} k (1-x)^n x^m$
(5)	$-r_A \equiv -dC_A/dt = -C_{A_0} k (1-x)(z+x)$

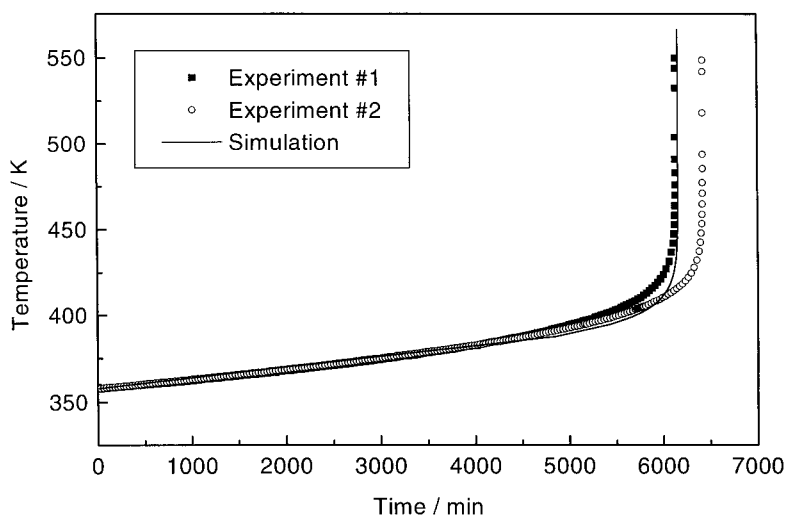


Fig. 2. Evolution of temperature during DCP decomposition in an ARSST unit. Simulated (continuous line) and experimental results.

activation energy is obtained from the temperature–time data can be explained by taking into account the heat losses and heat consumption by evaporation: these will reduce the rate of temperature increase (and therefore the calculated reaction rate) measured for a given temperature, which in an Arrhenius-type rate equation translates into a higher apparent activation energy. It can, therefore, be concluded that the more accurate value of the activation energy is the one obtained from concentration–time data in

isothermal experiments, which are not affected by heat losses.

The temperature–time data of Fig. 2 can be used to calculate  $T_{\text{onset}}$ . In our case, taking into account the detection limits of the system employed, an operational definition of  $T_{\text{onset}}$  was adopted as the temperature at which the exothermic activity is high enough to cause a 10% increase over the predetermined heating rate [6]. Since this rate is 0.25 K/min from 358 K upwards, from the previous definition  $T_{\text{onset}}$  corre-

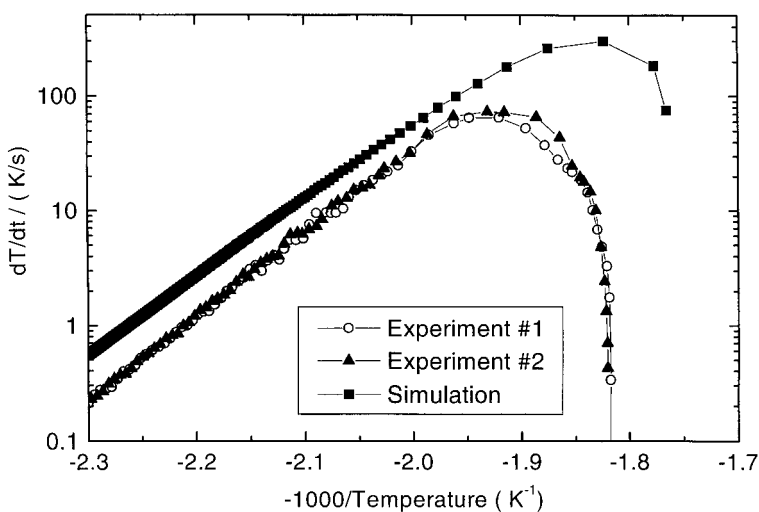


Fig. 3. Arrhenius plot of the self-heat rate obtained in the ARSST™. Simulated (continuous line) and experimental results.

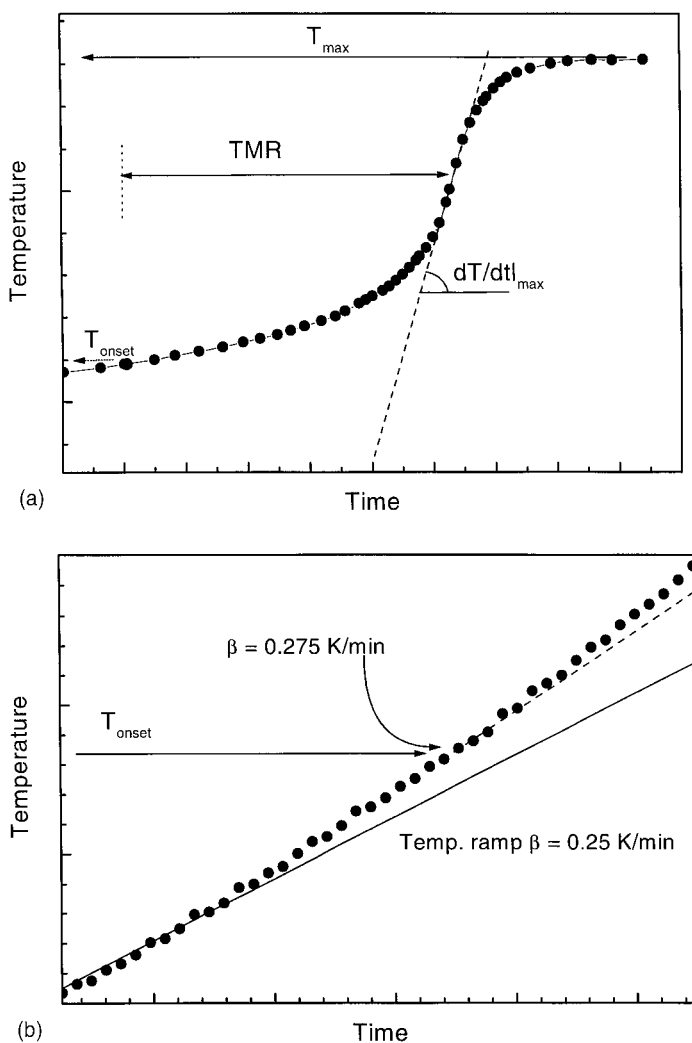


Fig. 4. (a): Diagram outlining the calculation of  $T_{\max}$ ,  $T_{\text{onset}}$ , TMR and  $(dT/dt)_{\max}$ . (b): Detailed calculation of  $T_{\text{onset}}$ .

sponds to the temperature existing in the ARSST<sup>TM</sup> cell when the measured heating rate exceeds 0.275 K/min. In addition to  $T_{\max}$  and  $T_{\text{onset}}$ , the simulations can also be used to calculate other runaway parameters such as the time to maximum rate (TMR) and the maximum rate of temperature increase  $(dT/dt)_{\max}$ . Fig. 4a illustrates these four parameters in a hypothetical runaway, and Fig. 4b details the calculation of  $T_{\text{onset}}$ . The calculated and experimental values for  $T_{\text{onset}}$ ,  $T_{\max}$ , TMR and  $(dT/dt)_{\max}$  are shown in Table 3. It can be seen that the predictions of  $T_{\max}$  are above, but relatively close to the experimental

Table 3

Runaway parameters: Comparison of model predictions and experimental data

	$T_{\max}$ (K)	$dT/dt_{\max}$ (K/min)	TMR (min)	$T_{\text{onset}}$ (K)
Experiment #1, ARSST <sup>TM</sup>	550	3919	102	382.1 <sup>a</sup>
Experiment #2, ARSST <sup>TM</sup>	550	4388	107	377.0
Simulation	566	18017	103	382.9

<sup>a</sup> $T_{\text{onset}}$  calculated in experiments carried out using the more accurate heat–wait–search operating mode.

Table 4  
Parameter values used in the parametric-sensitivity analysis

Parameter	Reference value	High value	Low value
Activation energy, $E_a$ (J/mol)	147429	162172	132686
Heat of reaction, $-\Delta H_r$ (J/mol)	290785	319864	261707
Pre-exponential factor, $A_0$ ( $s^{-1}$ )	$2.08 \times 10^{15}$	$2.29 \times 10^{15}$	$1.87 \times 10^{15}$
Specific heat of liquid, $h_{sl}$ (J/g K)	2.09	2.3	1.9

data, as already discussed. There is also a good agreement between the experimental and calculated values for TMR and  $T_{onset}$ . The only important deviation concerns  $(dT/dt)_{max}$ , where the model behaves conservatively, with theoretical  $(dT/dt)_{max}$  values that are considerably higher than the experimental ones. Again, a contributing factor to this difference may be the evaporative energy consumption during runaway, producing on slower temperature increase. It must also be noticed that  $(dT/dt)_{max}$  is the value subjected to a higher relative experimental error: it relies on temperature readings in an interval where the temperature undergoes a very rapid change.

### 3.3. Parameter sensitivity analysis

In the simulations discussed above, the kinetic parameters (activation energy and pre-exponential factor) were calculated either from concentration–time data in isothermal kinetic experiments or from

temperature–time data in dynamic ARSST<sup>TM</sup> experiments. In addition, the heat of reaction and the specific heat of the liquid sample were obtained from the literature or estimated using process simulators. Obviously, the error boundaries in these estimations have a direct effect in the characteristic magnitudes of the runaway:  $T_{onset}$ ,  $T_{max}$ , TMR and  $(dT/dt)_{max}$ . In order to assess the extent of this effect, a parameter sensitivity analysis has been carried out taking a  $\pm 10\%$  deviation (a typical error boundary) from the reference values given in Table 1. The new values are given in Table 4. The parametric analysis was carried out following standard methods [12]: the decomposition of DCP under a constant temperature ramp ( $\beta = 0.25$  K/min) was simulated to obtain the values of  $T_{onset}$ ,  $T_{max}$ , TMR and  $(dT/dt)_{max}$ . In each simulation, the value of one parameter was changed by  $\pm 10\%$ , while the rest were kept at their reference values.

Fig. 5 shows the sensitivity of  $T_{onset}$  with respect to the different system parameters. It can be seen that the

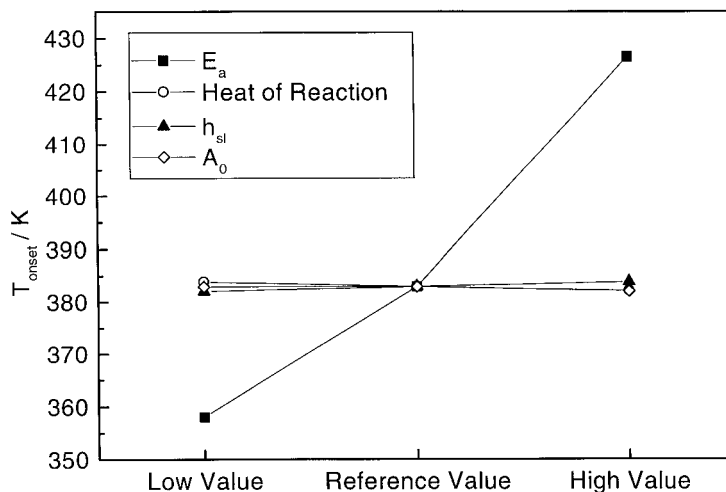


Fig. 5. Parametric sensitivity study. Influence of activation energy, pre-exponential factor, specific heat of the liquid and heat of reaction on  $T_{onset}$ .

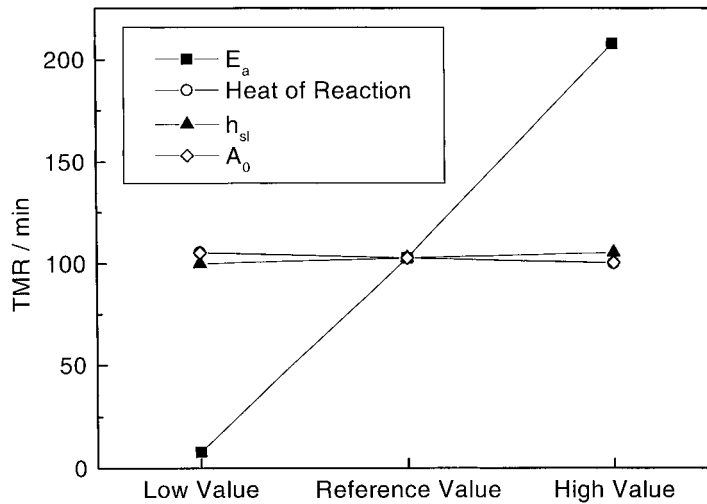


Fig. 6. Parametric sensitivity study. Influence of activation energy, pre-exponential factor, specific heat of the liquid and heat of reaction on TMR.

influence is minimal except for the activation energy, where going from the lower to the higher value (i.e. from  $0.9 \times E_a$  to  $1.1 \times E_a$ ) increases the value of  $T_{onset}$  by almost 70 K. The same can be said of TMR (Fig. 6): at the low value of the activation energy the runaway reaches the maximum rate almost immediately, while at the high value the runaway is delayed by ca. 200 min. This underlines the importance of an accu-

rate determination of the activation energy for simulation purposes: in the literature on kinetic studies, it is common to find variations of 10% and higher in the activation energy calculated by different authors for the same reaction system.

The variation of the maximum temperature  $T_{max}$  is also sensitive to the value of the activation energy, as shown in Fig. 7. This may seem surprising, since the

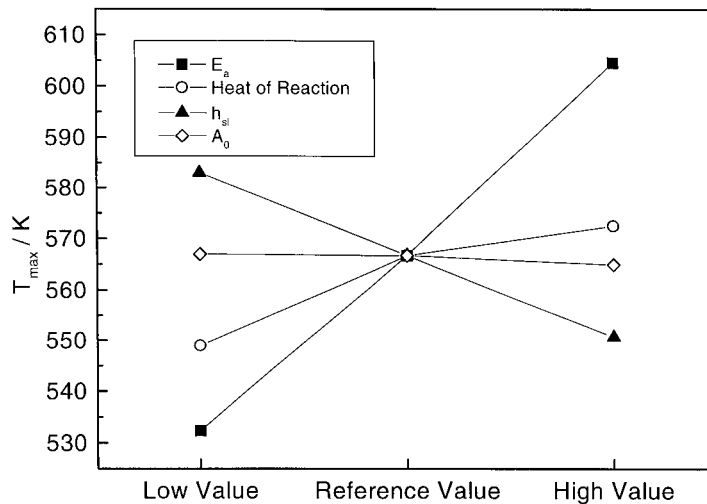


Fig. 7. Parametric sensitivity study. Influence of activation energy, pre-exponential factor, specific heat of the liquid and heat of reaction on  $T_{max}$ .



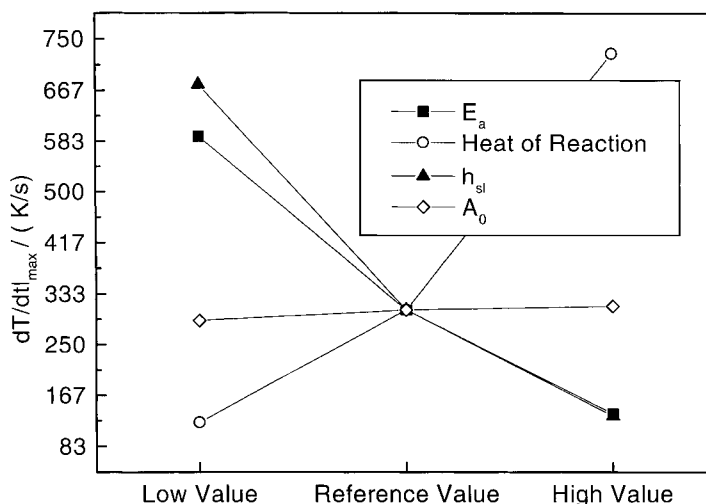


Fig. 8. Parametric sensitivity study. Influence of activation energy, pre-exponential factor, specific heat of the liquid and heat of reaction on  $(dT/dt)_{\max}$ .

model considers an adiabatic scenario without heat losses or evaporative cooling, and therefore  $T_{\max}$  should not be sensitive to changes in the reaction rate: an increase of the activation energy would delay the runaway, but not change the total heat released or the total temperature increase. However, it must be taken into account that the model simulates sample heating and subsequent runaway under a temperature ramp. Therefore, while runaway is being postponed by a higher  $E_a$ , the sample heating continues, and when the runaway finally occurs it starts at a higher temperature. Thus, the increase of  $T_{\max}$  in Fig. 7 corresponds well with the increase in  $T_{\text{onset}}$  shown in Fig. 5. Other influences on  $T_{\max}$  follow the expected trend:  $T_{\max}$  increases with the heat of reaction, decreases with the liquid specific heat and is little affected by the pre-exponential factor.

Finally, Fig. 8 illustrates the influence of the different parameters on the maximum heating rate,  $(dT/dt)_{\max}$ . As could be expected, the activation energy is also an important influence here, although the maximum effect on  $(dT/dt)_{\max}$  correspond to the heat of reaction: an increase from the low to the high value of  $-\Delta H_r$  increases  $(dT/dt)_{\max}$  from 122 to 727 K/s. This means that a small decrease in the value of  $-\Delta H_r$  used in the simulations would suffice to bring the predicted  $(dT/dt)_{\max}$  values in good agreement with the experi-

mental ones. Another important factor is the specific heat of the liquid, whose increase causes a strong decrease in the predicted value of  $(dT/dt)_{\max}$ . This opens up the possibility of mitigating the runaway of DCP decomposition by using a solvent of a higher heat capacity than ethylbenzene.

#### 4. Conclusions

The simplified model used in this work was able to predict with good accuracy the onset temperature, the maximum temperature and the time to maximum rate observed experimentally during the decomposition of DCP in ethylbenzene. The main deviation was observed in the maximum rate of temperature rise  $(dT/dt)_{\max}$ , where a more accurate prediction of the experimental results may require to account for evaporative losses during runaway, and perhaps also a more accurate determination of the specific heat of the liquid and the heat of reaction. These two parameters have only a limited effect on  $T_{\text{onset}}$ ,  $T_{\max}$  and TMR, but they exert a strong influence on  $(dT/dt)_{\max}$ .

The activation energy is the parameter with the strongest influence when modelling runaway reactions. An accurate determination of  $E_a$  is, therefore, vital to the predictive capacity of the simulation

model. In this work, the kinetics of DCP decomposition were obtained from concentration–time data gathered in independent isothermal experiments. Unlike temperature–time data gathered in reaction calorimeters, these results were exempt from interference from spurious factors such as evaporative cooling, heat losses and temperature inhomogeneities in the reaction vessel. Thus, concentration–time data lead to a more reliable determination of the kinetics of decomposition (activation energy and pre-exponential factor), and should be employed when the system characteristics allow its use.

### Acknowledgements

Research on reactor safety at the University of Zaragoza is carried out with financial support from Fundacion MAPFRE, and from Diputación General de Aragón (DGA), Spain; Project P71/97.

### References

- [1] J.L. Gustin, *J. Loss Prev. Process Ind.* 6 (5) (1993) 275.
- [2] A.Y. Tonkovich, J.L. Zilka, M.J. LaMont, Y. Wang, R.S. Wegeng, *Chem. Eng. Sci.* 54 (1999) 2947–2951.
- [3] A. Keller, D. Stark, H. Fierz, E. Heinzle, K. Hungerbühler, *J. Loss Prev. Ind.* 10 (1) (1997) 31.
- [4] J. Sempere, R. Nomen, R. Serra, P. Cardillo, *J. Loss Prev. Proc. Ind.* 10 (1) (1997) 55.
- [5] S. Tharmalingham, *The Chemical Engineer*, 1989.
- [6] E. Marco, J.A. Peña, J. Santamaría, *Chem. Eng. Sci.* 52 (1997) 3107–3115.
- [7] A. Kossoy, E. Koludarova, *J. Loss Prev. Process Ind.* 8 (4) (1995) 229–235.
- [8] J. Zawadiak, D. Gilner, Z. Kulicki, S. Baj, *Analyst* 118 (1993) 1081.
- [9] A. Kossoy, V. Belochvostov, J.L. Gustin, *J. Loss Prev. Proc. Ind.* 7 (5) (1994) 397.
- [10] Proceedings DIERS users group meeting, Boston, MA, 1994.
- [11] R.B. Seymour, C.E. Carraher, *Seymour/Carraher Polymer's Chemistry*, Marcel Dekker, 1996.
- [12] G.E.P. Box, W.G. Hunter, J.S. Hunter, *Statistics for Experimenters*, Wiley Interscience, New York, 1978.